AATCC Review

15 October 2024: Received
10 January 2024: Revised
07 February 2025: Accepted
11 February 2025: Available Online

https://aatcc.peerjournals.net/

Original Research Article

Open Access

Green Synthesis of Silver Nano particles and Assessment of their In-Vitro Antibacterial Potential Against Common Pathogens in Bovine Semen

Arushi Kanwar[1], Meenakshi Virmani[1*], Sant Lal[2], Rajesh Kumar[1], Sandeep Kumar[3], Kartik Chaudhary[4]

[1]*Department of Veterinary Physiology and Biochemistry, Lala Lajpat Rai University of Veterinary and Animal Sciences, Hisar, Haryana, (125004) India*
[2]*PhD Scholar, Division of Bio and Nano Technology, Guru Jambheshwar University of Science and Technology, Hisar, Haryana, India*
[3]*Department of Veterinary Gynaecology and Obstetrics, Lala Lajpat Rai University of Veterinary and Animal Sciences, Hisar, Haryana, (125004) India*
[4]*Forest Department-Wildlife Wing, Paonta Sahib, Himachal Pradesh, India*

ABSTRACT

Bacterial contamination in bovine semen significantly impacts fertility and overall health in the cattle industry. Traditional antibiotics used to control this contamination raise concerns about antibiotic resistance and potential adverse effects on sperm quality. This study explores the use of green-synthesized silver nanoparticles (AgNPs) as an alternative antibacterial agent for semen preservation. AgNPs were synthesized using ethanolic extracts of Withania somnifera (ashwagandha) and Syzygium aromaticum (clove) and their antibacterial efficacy was evaluated against common semen pathogens. The synthesized AgNPs displayed superior antibacterial activity, particularly those derived from ethanolic extracts, which were further characterized for their size, shape, stability, and crystalline structure. UV-Vis spectroscopy, Zeta potential measurements, TEM, XRD, and FTIR analyses confirmed the formation of stable, spherical AgNPs with desirable properties for application in semen extenders. This study highlights the potential of green-synthesized AgNPs as a sustainable and effective alternative to antibiotics for reducing bacterial contamination in cryopreserved semen, mitigating the risk of antibiotic resistance.

One significant challenge of the study is the variability in the synthesis and characterization of AgNPs, which may affect their antibacterial efficacy and stability. Additionally, the potential long-term effects of AgNPs on sperm quality and fertility require thorough investigation to ensure their safety in practical applications.

Despite these challenges, the study contributes significantly to the cattle industry by offering a sustainable and effective method to combat bacterial contamination in cryopreserved semen. By demonstrating the superior antibacterial activity of AgNPs synthesized from natural extracts, this research paves the way for reducing reliance on traditional antibiotics, thereby addressing concerns related to antibiotic resistance and enhancing overall reproductive health in cattle.

Keywords: *Green synthesis, silver nanoparticles, antibacterial activity, semen, pathogens, ashwagandha, clove, characterization, etanolic extract, aquous extracxt*

1. Introduction

Although various genetic, health, and environmental factors have been linked to decreased fertility in the cattle industry, bacterial contamination of bovine semen can also significantly contribute to reduced birth rates and bovine health complications [1]. Recent studies on humans and vertebrate animals indicate that the reproductive microbiome plays a crucial role in reproductive health and fertility [2]. The presence of bacteria in ejaculates may originate from intrinsic bacteriocins within the male urogenital tract, extending from the testes to the penile foreskin [3]. Even with stringent hygiene protocols during semen collection, ubiquitous bacteria can still originate from sources such as the artificial vagina, laboratory glassware and equipment, semen extenders, and even the laboratory environment [4].

Corresponding Author:* ***Meenakshi Virmani*

DOI: https://doi.org/10.21276/AATCCReview.2025.13.01.286

Although opportunistic pathogens like *Staphylococcus, Streptococcus, Mycoplasma, Pseudomonas, Corynebacterium*, and *Bacillus* can be present even in ejaculates from clinically healthy bulls [5,6]. Bacterial contamination of extended semen has been linked to reduced sperm motility [7] and viability [8], acrosomal damage [9] and sperm agglutination [10]. Bacteria found in semen have been shown to provoke a local immune response. This immune defense is supported by the infiltration of leukocytes, which results in the production and secretion of cytokines. Such events have been linked to a decrease in male reproductive potential [11]. Semen intended for artificial insemination (AI) must be free of infectious agents. To prevent bacterial contamination, including mycoplasmas, various types of antibiotics have been incorporated into seminal extenders before freezing. Antibiotics such as amikacin, ofloxacin, and gentamicin have demonstrated high efficacy against bacteria such as Pseudomonas aeruginosa and Acinetobacter species isolated from frozen semen [12]. Additionally, the combination of benzylpenicillin and streptomycin has been found to significantly lower bacterial load while preserving sperm motility and integrity [13, 14]. Although they offer benefits, the non-therapeutic use of antibiotics raises concerns regarding sperm quality and the potential for antibiotic resistance [15].

Recent scholarly discourse underscores the necessity of exploring alternatives to antibiotics in semen extenders to adhere to safe usage recommendations in veterinary practices [15]. The utilization of antibiotics in semen during cryopreservation raises significant concerns regarding antibiotic resistance. Research has shown that traditional antibiotics, although effective against specific bacteria, contribute to the emergence of resistant strains. For example, one study discovered that 22% of the microorganisms isolated from bull semen exhibited resistance to commonly used antibiotics [16]. Furthermore, excessive use of antibiotics in semen processing can result in heightened resistance among both male partners and the bacterial flora in the embryo culture system during IVF [17]. This underscores the necessity for alternative approaches to mitigate bacterial contamination without exacerbating antibiotic resistance. Various strategies have been investigated, including the use of plant-based substances, antimicrobial peptides, and physical methods to reduce bacteria. Curcumin extract has shown promise in decreasing bacterial counts while preserving sperm viability [18]. Honey has also been assessed for its antimicrobial properties and has proven effective in maintaining buffalo bull spermatozoa [19]. Furthermore, antimicrobial peptides [20] and nanoparticles [21] have emerged as effective alternatives for controlling bacterial growth without compromising sperm quality [22, 23]. Techniques such as single-layer centrifugation and colloidal centrifugation effectively separate bacteria from sperm, thereby enhancing the sample quality [18, 23]. These alternatives not only reduce the risk of antibiotic resistance but also enhance overall fertility outcomes in artificial insemination practices. Green-synthesized silver nanoparticles (AgNPs) have been identified as potential antibacterial agents against a range of Gram-positive and Gram-negative pathogenic bacteria. These include bacteria such as *Salmonella epidermidis, Streptococcus pyogene, Vibrio parahaemolyticus* [24], *Staphylococcus aureus, Escherichia coli* [25], *Pseudomonas aeruginosa, Bacillus cereus* [26]. In this study, we synthesized green silver nanoparticles using ethanolic extracts of *Withania somnifera* (ashwagandha) powder and clove (*Syzygium aromaticum*) bud powder and evaluated their antibacterial activity for potential application as effective antibacterial agents in cryopreserved semen. This innovative approach aims to replace conventional antibiotics, offering a more sustainable and effective solution for combating bacterial contamination in semen, without the risk of developing antibiotic resistance.

2. Materials and Methods

2.1.1 Preparation of Ethanolic Ashwagandha Extract

AgNPs were synthesized *using* ashwagandha extract (EA-AgNP). A 0.2% ethanol extract of ashwagandha was prepared by dissolving 0.2 g of ashwagandha in 100 ml of ethanol. The mixture was stirred for 1 h at 800 rpm and 40°C. Following stirring, the extracts were centrifuged at 5000 rpm for 15 min, and the supernatants were collected.

A 6.5 mM solution of silver sulfate was prepared by dissolving 0.20267 g of silver sulfate in 100 ml of double-distilled water. Ten milliliters of this solution were placed in a conical flask on a magnetic stirrer at 800 rpm for 10 min at 60°C. After 10 min, 5 ml of each ashwagandha extract was added dropwise to the silver sulfate solution. The mixture was then stirred for an additional 30 min. The pH of the solution was adjusted to 9 using 1N NaOH. After 10 min, the UV absorption of the solutions was measured using a spectrophotometer.

2.1.2 Preparation of EthanolicClove Extract

AgNPs were synthesized using an ethanolic clove extract (EC-AgNP). An aqueous clove extract (0.2%) was prepared by dissolving 0.2 g of clove powder in 100 ml of ethanol. The mixtures were stirred for 1 hour at 800 rpm and 40°C. Following stirring, the extracts were centrifuged at 5000 rpm for 15 minutes, and the supernatants were collected.

A 6.5 mM solution of silver sulfate was prepared by dissolving 0.20267 g of silver sulfate in 100 ml of double-distilled water. Ten milliliters of this solution were placed in a conical flask on a magnetic stirrer at 800 rpm for 10 minutes at 60°C. After 10 min, 3 ml of each clove extract was added dropwise to separate the silver sulfate solutions. The mixtures were stirred for an additional 30 minutes. The pH of the solutions was adjusted to 9 using 1N NaOH. UV absorption of the solutions was measured using a spectrophotometer after 10 minutes.

2.1.3Post-Synthesis Processing of Nanoparticles

The synthesized nanoparticles were centrifuged at 12,000 rpm for 20 min. The supernatant was decanted and the pellet was washed with distilled water by vortexing. The samples were centrifuged again at 12,000 rpm for 20 minutes. This washing process was repeated three times, and the final pellet was collected in a Petri dish and dried at 60-70°C on a hot plate. The dried nanoparticles were then used for various characterization and applications.

2.2Characterization of Silver Nanoparticles

2.2.1 Particle size analysis

The size of the synthesized nanoparticles was measured using a Zetasizer Nano ZS (Malvern Instruments Ltd., UK, Model Micro-P, range 0.05-550 microns) with Dynamic Light Scattering (DLS)

2.2.2 Transmission Electron Microscopy

(TEM) was performed using a JEM-2100 HRTEM to determine the shape and size of the nanoparticles. TEM samples were prepared by drop-casting the nanoparticle dispersion onto a carbon-coated copper grid and drying completely. The samples were examined at a potential of 20 kV, with a point resolution of 0.2 nm and a lattice resolution of 0.14 nm.

2.2.3 Zeta potential

The zeta potential, which indicates the degree of electrostatic repulsion between adjacent similarly charged particles, was determined in millivolts using a Zetasizer Nano ZS with Electrophoretic Light Scattering (ELS).

2.2.4 X-ray diffraction

A (XRD) patterns were measured using a Rigaku MiniFlex600 instrument to investigate the crystal structure, phase purity, and lattice parameters of the nanoparticles. Surface morphology and elemental analyses were performed using Scanning Electron Microscopy (SEM) with a ZEISS EVO MA10. Crystallite sizes were estimated using Scherrer's method from the powder XRD data obtained using Bruker Axes D-8.

2.2.5 Fourier Transform Infrared

(FTIR) spectra were recorded using a Perkin Elmer 2000 Optica model (spectral range of 10000 cm−1 to 370 cm−1) over the range of 4000–400 cm−1.

2.2.6 Raman spectroscopy

It was conducted using an Airix Raman spectrometer to analyze the vibrational modes and assess the characteristic peaks indicative of the molecular composition and structure. Raman spectra provided insights into vibrational properties, confirming the chemical and structural integrity of the nanoparticles.

2.2.7 Fourier Transform Infrared Spectroscopy

FTIR analysis was performed to reveal the potential biomolecules involved in surface coating and as capping agents to stabilize NP. Additionally, this analysis helped identify the functional groups present in the suspension of AgNPs, which may be responsible for the reduction of metal ions. The images show different stretches of the bonds at different peaks. The sample was screened using an FTIR spectrophotometer in the 400–4,000 cm^{-1} range to determine the chemical interaction of NPs with phytochemicals from Ashwagandha and clove.

2.3 Evaluation of Antibacterial Activity of Nanoparticles

The antimicrobial activity of aqueous and ethanolic nanoparticles was determined using the agar well diffusion method [33]. Muller Hilton agar (MHA) was prepared by dissolving 38 grams of MHA powder in 1000 ml of water, autoclaving at 121°C for 15 minutes at 15 psi, and cooling. The agar was poured into petri plates (60 mm in diameter) and left undisturbed for 30 minutes to solidify.

The agar plate surface was inoculated by spreading a microbial inoculum of *Escherichia coli* (MTCC 38), *Staphylococcus aureus* (Fop 171A), *Streptococcus dysgalactiae* (MTCC 5101), and *Pseudomonas pseudoalcaligenes* (MTCC 5210) over the entire agar surface. Wells of 6 mm diameter were punched aseptically, and 50 µl of silver nanoparticles formed from ethanolic extracts of ashwagandha and clove were introduced into the wells. The agar plates were incubated at 37°C for 24 hours. The zone of inhibition, indicating antimicrobial activity, was measured using vernier calipers.

3. RESULTS

3.1 Green synthesis of silver nanoparticles

10mL of 6.5 mM solution of silver sulfate was combined with a 0.2% ethanolic extract of ashwagandha root powder. The mixture was heated to 60°C and stirred continuously at 800 rpm. The ashwagandha extract successfully reduced Ag^{+} ions to Ag^{0}, as evidenced by a visible color change in the solution, confirming the initial step of green synthesis of silver nanoparticles. To adjust the pH, NaOH was added, resulting in the solution turning brown (figure 1).

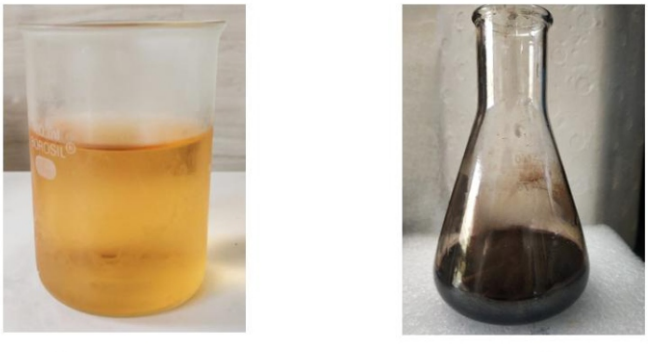

A B

Figure 1: Colour change indicating formation of silver nanoparticles (A) Extract (B) Prepared nanoparticles

3.2 Characterization of silver nanoparticles

3.2.1 UV-Vis spectroscopic analysis

UV-Vis spectroscopic analysis of biosynthesised silver nanoparticles was performed by continuous scanning from 350 to 700 nm and 1 mM silver sulphate solution was used for baseline correction. Spectra of silver colloids contained strong plasmon band close to 434 nm wavelength in case of EA-AgNPs (Figure 2) and 430 nm in case of EC-AgNPs (Figure 3), which confirmed the reduction of silver ions (Ag^{+}) to silver nanoparticles (Ag°).

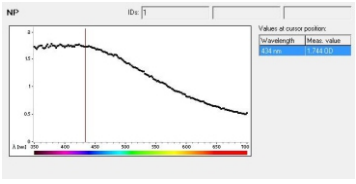

Figure 2a: UV-Vis spectrum for EA-AgNPs

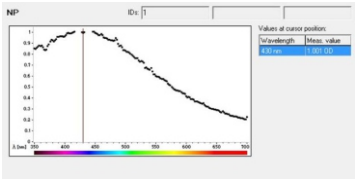

Figure 2b: UV-Vis spectrum for EC-AgNPs

Measurement of particle size reflects the success of the technique employed during preparation of nanoparticles. Zetasizer Nano ZS was used to measure the particle size of dispersed nanoparticles in nanometers, using the technique of Dynamic Light Scattering (DLS).

Particle Size Analysis (PSA) data for silver nanoparticles synthesized using ethanolic Ashwagandha extract (Figure 4) indicated that the nanoparticles have an average size of approximately 216.3 nm with a moderate distribution in size (PDI = 0.358). The resulting quality is considered good, and the size distribution graph shows a sharp peak at 185.8 d.nm, confirming that the sample consisted of nanoparticles mainly around this size. The single peak in the size distribution graph suggests a relatively uniform size distribution, which is desirable for many applications of nanoparticles. These findings suggest that Ashwagandha extract is effective in synthesizing silver nanoparticles with a consistent size distribution, which could be beneficial for their intended applications.

The PSA data for silver nanoparticles synthesized using clove extract (Figure 5) indicates that the nanoparticles have an average size of approximately 212.2 nm with a moderate distribution in size (PDI = 0.358). The resulting quality is considered good, and the size distribution graph shows a sharp peak at 175.6 nm, confirming that the sample consists mainly of nanoparticles around this size. The single peak in the size distribution graph suggests a relatively uniform size distribution, which is desirable for many applications of nanoparticles. These findings suggest that clove extract is effective in producing nanoparticles with a consistent size distribution

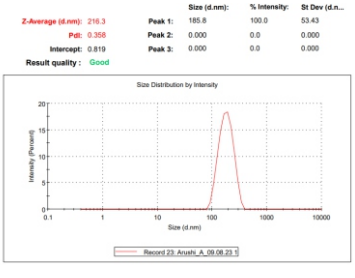

Fig. 3a: PSA of EA-AgNPs

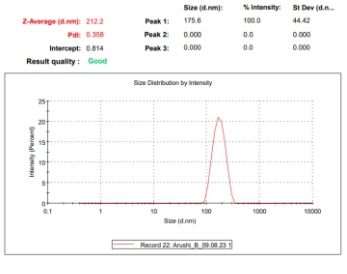

Figure 3b: PSA of EC-AgNPs

Zeta potential refers to the electrical charge that forms at the interface between a solid surface and the surrounding liquid. It represents the surface charge of nanoparticles when suspended in a solution.

This measurement is essential to assess the condition of the nanoparticle surface and predict the stability of formed nanoparticles in colloidal solution mixture. Its value ranges between -60 to +60 mV and values between -30 to +30 mV are considered to be more stable [27]. The zeta potential was recorded to be -22.8 mV and -18 mV for EA-AgNPs(figure 6) and EC-AgNPs (figure 7) respectively. This indicates that the biosynthesized silver nanoparticles were stable and did not coagulate.

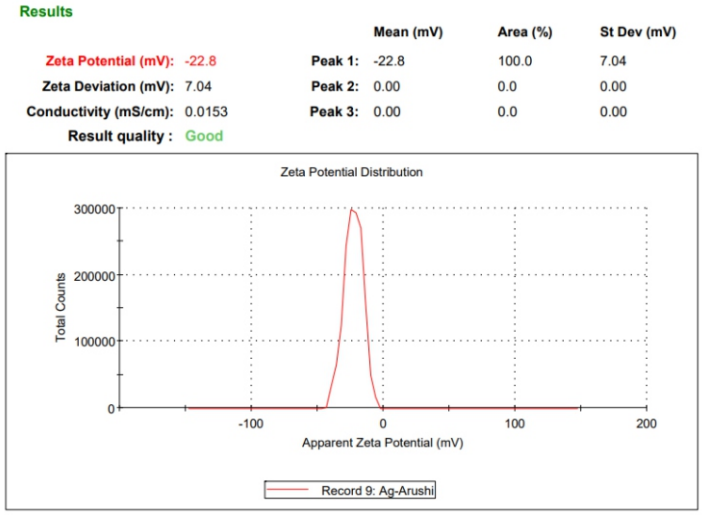

Figure 4a: Zeta Potential of EA-AgNPs

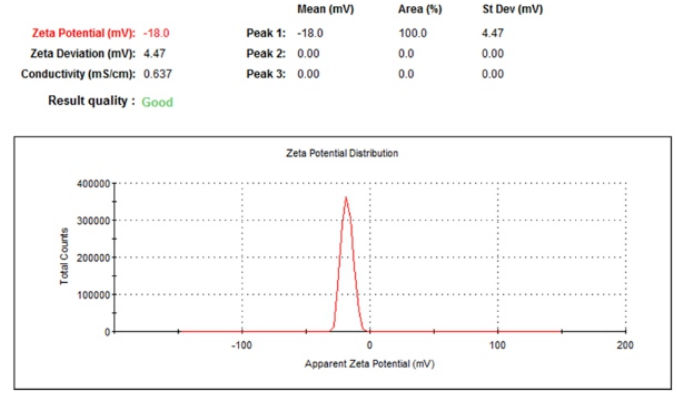

Figure 4b: Zeta potential of EC-AgNPs

3.2.4 TEM

The TEM images of EA-AgNPs (Figure 8) at 20 nm scale showed that the particle size of biosynthesized nanoparticles ranged from 4.78 nm to 20.97 nm. The nanoparticles appeared to be roughly spherical, with some having slightly irregular shape. The particles seemed to be dispersed across the grid with some areas showing clustering.

The TEM analysis of EC-AgNPs (Figure 9) showednanoparticles of size varying from 16 nm to 34 nm at 20nm scale. The biosynthesized nanoparticles were roughly spherical, although some were irregularly shaped. Some nanoparticles appeared to be clustered together, indicating little aggregation.

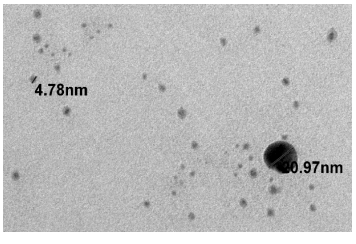

Figure 5b: TEM image of EC-AgNPs extract

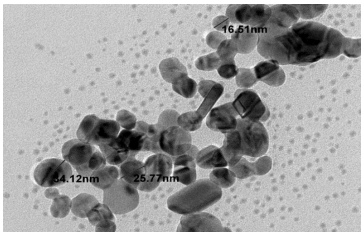

Figure 5a: TEM image of EA-AgNPs

3.2.5 X-ray diffraction (XRD) pattern

The X-ray diffraction (XRD) pattern of the biosynthesized silver nanoparticles using ashwagandha extract (figure 10) was recorded by using x ray diffractometer. XRD pattern of EA-AgNPs is shown in Figure 12. Data was collected at a step of 0.0202 degrees for the 2θ range of 30 to 80°. Four peaks at 2θ values of 38.02°, 44.21°, 64.41° and 77.43° identified in the diffractogram correspond to (hkl) values – (1 1 1), (2 0 0), (2 2 0) and (3 1 1) planes due to silver metal. Ag nanoparticle formation was evident from the intense X-ray diffraction pattern. The crystalline nature of Ag Nanoparticles was confirmed by X-ray diffraction analysis. The high degree of crystallinity is reflected in the peak intensity. Thus, XRD analysis has confirmed that the prepared sample contains silver nanoparticles with the face-centered-cubic crystal structure.

XRD pattern of the as-synthesized silver nanoparticles from clove extract is shown in figure 11. The X-ray diffraction pattern (XRD) of synthesized the as silver nanoparticles were recorded by using x ray diffractometer.Data was collected at a step of 0.0202 degrees for the 2θ range of 30 to 80°. Ag nanoparticles synthesized from clove extract exhibited diffraction peaks at 38.2°, 44.2°, 64.4° and 77.4° which were indexed with diffraction planes (1 1 1), (2 0 0), (2 2 0) and (3 1 1) due to silver metal. Ag nanoparticle formation was evident from the intense X-ray diffraction pattern. The crystalline nature of Ag Nanoparticles was confirmed by X-ray diffraction analysis. The high degree of crystallinity is clearly reflected in the peak intensity. Thus, XRD analysis has confirmed that the prepared sample contains silver nanoparticles with cubic crystal structure and face-centered crystallization.

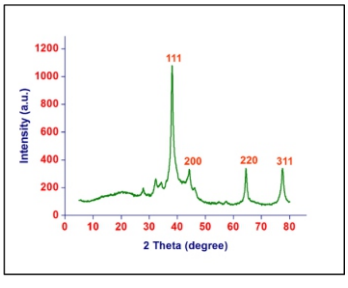

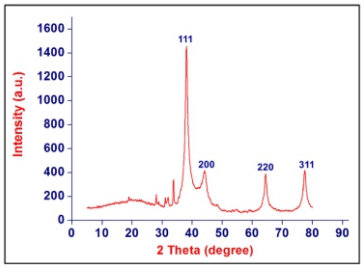

Figure 6a: XRD profile of EA-AgNP Figure *6b. XRD profile of EC-AgNP*

3.2.6 Field Emission- Scanning Electron Microscopy

This Field Emission Scanning Electron Microscopy (FESEM) image shows the morphology and size distribution of ethanolic Ashwagandha nanoparticles (Figure 12). The nanoparticles exhibit a generally spherical shape with some degree of aggregation. The surface appears rough, which might be due to the intrinsic properties of the Ashwagandha nanoparticles. The image reveals clusters of nanoparticles, possibly indicating agglomeration, which is common in nanoparticles due to van der Waals forces and other interactions [28].The scale bar at the bottom right indicates 200 nm, allowing for a rough estimation of particle size. The individual particles in the image seem to range from smaller than 100 nm to around 200 nm in diameter.

The nanoparticles formed using ethanolic clove extract (Figure 13) predominantly exhibit a spherical shape, which is consistent with many nanoparticle formations. There is a noticeable degree of aggregation, with particles clustering together. The scale bar in the image indicates 500 nm, allowing for the estimation of particle sizes.Individual particles in the image range from approximately 50 nm to 300 nm in diameter. This size range is typical for nanoparticles and is consistent with what might be expected from ethanolic plant extract-based

synthesis. The variation in size suggests a polydisperse nature of the nanoparticle sample. The image reveals significant cluster formation, with nanoparticles tending to aggregate into larger groups.This clustering behavior may be due to several factors such as solvent evaporation during sample preparation for FESEM imaging, inherent properties of the ethanolic clove extract used in nanoparticle synthesis or possible interactions between the nanoparticles themselves, such as electrostatic or van der Waals forces [29].

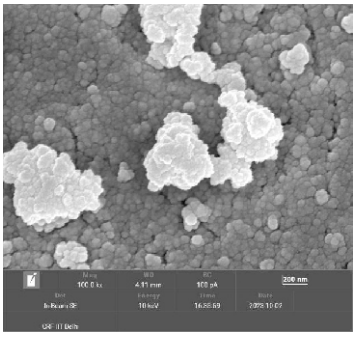

Figure 7a: FE-SEM silver NP prepared using ethanolic ashwagandha extract showing cauliflower shape of as synthesised NP

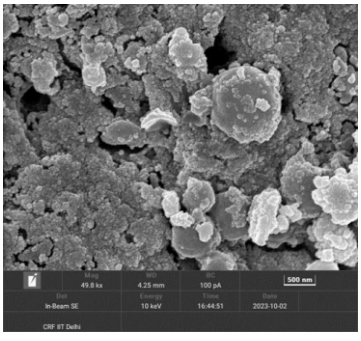

Figure 7b: FE-SEM silver NP prepared using ethanolic clove extract showing cauliflower shape of as synthesised NP

Raman spectra of silver nanoparticles synthesized using ashwagandha extract and clove extract are shown in figure 14 (A)and 16(B), respectively.

Ag nanoparticles synthesized using ashwagandha extract exhibited vibrational modes at 252.14 cm^{-1}, 647 cm^{-1}, 1317 cm^{-1}, 1395.11 cm^{-1} and 1585.40 cm^{-1} , while Ag nanoparticles synthesized using clove extract displayed the peaks at 464.18 cm^{-1}, 633.79 cm^{-1}, 1353.87 cm^{-1} and 1579.42 cm^{-1}.

Due to the stretching vibration of C-N-C and C-S-C, the Raman spectra of Ag NPs_1 exhibited peak at 647 cm^{-1}, while the spectra of Ag NPs_2 displayed the peaks at 464.18 cm^{-1} and 633.79 cm^{-1} [30].The spherical shape of silver nanoparticles may be the reason for unremakeble peaks in the raman spectra [31].

The other significant vibrational peaks at 1317 cm^{-1}, 1395.11 cm^{-1} and 1585.40 cm^{-1} in case of ashwagandha NP's, while at 1353.87 cm^{-1} and 1579.42 cm^{-1} in case of clove NP's were produced due to carboxylic symmetric and anti-symmetric C=O stretching vibration of the carboxylic group, respectively. These significant peaks are specific to silver nanoparticles [30].

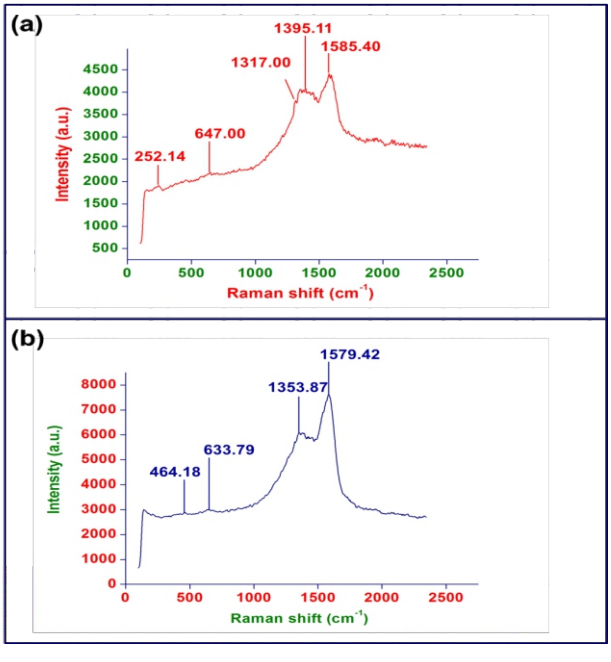

Figure 8. Raman spectra of silver nanoparticles: (A) synthesized using ashwagandha extract and (B) synthesized using clove extract

3.2.8 Fourier-transform infrared (FTIR) spectroscopy

The FTIR spectra of AgNPs synthesized using the Ashwagandha (Figure 15) produced peaks at 616.38, 803.46, 1025, 1077.08, 1383.35, 1620.70, 2920.29 and 3419.63 $^{cm-1}$. The peak at 3,419 cm−1 is due to stretching vibrations of O–H, attributing the presence of phenolic and alcoholic groups on the surface of AgNPs. Other peaks at 2920.29 $^{cm-1}$ are attributed to the C–H stretching vibration of alkanes. The peak at 1,620.70 $^{cm-1}$ is attributed to C–O bond vibrations and C–C stretching vibrations. The peaks at 1,383.35 correspond to the C–H bending of alkanes and C–O stretching in the carbonyl group of protein residues. Two other peaks at 1,077.08 and 1,025 $^{cm-1}$ may indicate the C-stretching of ether groups, the C–N stretching vibration of aliphatic amines, and the C–O vibration. Stretching vibrations of C–X of alkyl halides were observed at 803.46 cm^{-1}. The vibration of aromatic ring in Ashwagandha extract can be seen at 616 cm^{-1}. The result of the FTIR analysis substantiated the role of extract as capping agent in the formation of Ag NPs.

The FTIR spectra of AgNPs synthesized using the clove extract (Figure 16) produced peaks at 441.11, 616.38, 1375.53, 1632.52, 2321.77. 2847.56 and 2917.47^{cm-1}. Absorbance bands at 441.11^{cm-1} is likely due to metal-oxygen bonds, confirming the presence of silver nanoparticles indicating that the functional groups present in the clove extract (likely phenolic compounds such as eugenol) are interacting with the surface of the silver nanoparticles, functioning as capping agents and stabilizing the nanoparticles. Peak at 616.38 $^{cm-1}$ can be attributed to C-Cl stretching vibrations, indicating the presence of alkyl halides. 1375.53 corresponds to the N-O symmetric stretching vibrations, which are characteristic of nitro compounds, widely present in S. aromaticum extract. The absorbance band at 1631.68 cm−1 corresponds –CO-stretch formed in eugenol after the bioreduction process. 2321 $^{cm-1}$ peak may be associated with C≡N stretching vibrations, suggesting the presence of nitriles.The bands at 2847.56 cm−1 and 2917.47 cm−1 represent C–H stretching of alkanes. band at 3419.63 $^{cm-1}$ is due to O–H group of residual eugenols. These peaks collectively indicate that various functional groups such as alcohols, phenols, alkanes, nitriles, ketones, aldehydes, carboxylic acids, nitro compounds, and alkyl halides are involved in the stabilization and coating of silver nanoparticles formed using clove extract.

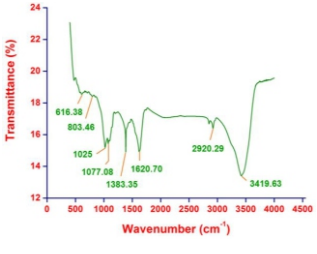

Figure 9a. FTIR of EA-AgNP Figure

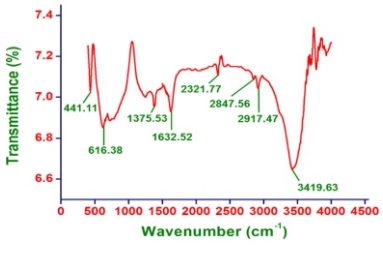

9b. FTIR of EC-gNP

3.3 Evaluation of antibacterial activity of biosynthesized silver nanoparticles

Antimicrobial activity of of AgNPs *viz.,* ethanolic ashwagandha AgNP& ethanolic clove AgNPswas determined by agar well diffusion method against *Escherichia Coli, Staphylococcus aureus, Streptococcus dysgalactiae* and *Pseudomonas pseudoalcaligenes* (Fig. 17*)*. Diameter of zone of inhibitions were measured (in mm) after 24 hours of incubation at 37º C to determine the antibacterial activity (Table 1, 2, 3, 4).

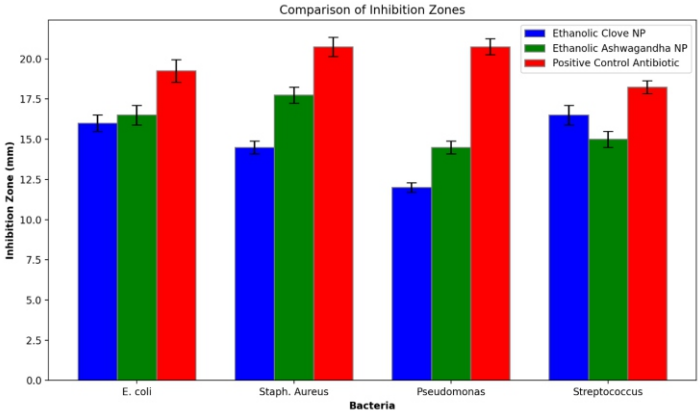

Figure 10: Bar graph of antimicrobial activity

Discussion

The study aimed to evaluate the antimicrobial efficacy of green-synthesized silver nanoparticles against pathogens found in bovine semen. The results demonstrated a significant reduction in bacterial load, suggesting that these nanoparticles could serve as a potent antimicrobial agent in the cattle industry.

Comparison with Previous Studies

Ag NPs can be synthesized using various plant extracts, such as jackfruit and Sempervivum tectorum, which act as reducing agents. This method is environmentally friendly and cost-effective [32,33]. Techniques like UV-Vis spectroscopy, X-ray diffraction, and scanning electron microscopy are employed to confirm the size, shape, and crystalline structure of the synthesized nanoparticles [33,34]

Our findings align with previous research indicating the effectiveness of silver nanoparticles as antimicrobial agents [35]. The green synthesis approach not only provides an eco-friendly alternative but also enhances the biocompatibility of the nanoparticles, as supported by studies such as those by Ahmed *et al*.,2016 [36].

Mechanism of Action

The antimicrobial activity of silver nanoparticles is primarily attributed to their ability to disrupt bacterial cell membranes and interfere with cellular processes [37].

Ag NPs interact with bacterial cell walls and membranes, leading to structural damage and the generation of reactive oxygen species (ROS), which contribute to their antimicrobial effects [38]. Studies have shown that Ag NPs are effective against both gram-positive and gram-negative bacteria, including multidrug-resistant strains [8]. While the antibacterial properties of green synthesized Ag NPs are promising, concerns about potential microbial resistance and the need for further research into their long-term effects and safety remain critical for their application in medicine [38].

Implications for the Cattle Industry

The application of green-synthesized silver nanoparticles could revolutionize the cattle industry by reducing the incidence of bacterial contamination in semen, thereby improving fertility rates and overall bovine health. This aligns with the findings of [1], who highlighted the impact of bacterial contamination on fertility. The application of green-synthesized silver nanoparticles (AgNPs) in the cattle semen industry presents a promising avenue for enhancing reproductive health and disease management.

The eco-friendly synthesis of AgNPs provides nanoparticles with significant antibacterial properties, which can be beneficial in preserving semen quality and preventing microbial contamination during storage and transport [30, 31]. The incorporation of AgNPs in semen extenders can potentially enhance

sperm viability and motility by reducing microbial load, which is essential for successful artificial insemination [30]. Utilizing green synthesis methods aligns with sustainable agricultural practices, promoting environmental health while improving livestock productivity [32].

Limitations and Future Research

While the results are promising, further research is needed to assess the long-term effects and safety of these nanoparticles in vivo. Additionally, exploring the synergistic effects of silver nanoparticles with other antimicrobial agents could provide insights into more effective treatment strategies.

Conclusion

In conclusion, green-synthesized silver nanoparticles exhibit significant antimicrobial potential against semen pathogens, offering a sustainable and effective solution for improving reproductive health in cattle.

Future Scope of Study

The promising results of green-synthesized silver nanoparticles (AgNPs) and their antibacterial efficacy in bovine semen open new research opportunities:

1. Long-Term Safety: Conduct in vivo studies to assess AgNPs' long-term effects on sperm quality, fertility, and health, including tissue accumulation.

2. Mechanistic Insights: Investigate how AgNPs interact with bacteria, generate reactive oxygen species (ROS), and elicit cellular responses.

3. Synergy with Antimicrobials: Explore AgNPs combined with other agents or natural extracts to enhance efficacy and reduce antibiotic resistance risks.

4. Formulation Advances: Optimize AgNP integration into semen extenders, focusing on stability, sperm motility, and cryopreservation impacts.

5. Field Trials: Test AgNPs in commercial cattle operations to assess fertility and herd health in real-world applications.

6. Alternative Plant Sources: Identify new antimicrobial plant sources for AgNP synthesis to broaden antibacterial effectiveness.

7. Regulation and Ethics: Establish guidelines for AgNP use, ensuring safety, compliance, and animal welfare.

8. Microbiome Impact: Study AgNPs' effects on the reproductive microbiome to balance beneficial and harmful microbes.

Future research in these areas can improve strategies for bacterial control in bovine semen, boosting reproductive health and cattle productivity.

Conflict of interest

Authors declare no conflict of interest

Acknowledgment

We are grateful to Lala Lajpat Rai University of Veterinary and Animal Sciences for providing resources for this study.

Table 1: Antibacterial activity against *Staph. aureus*	Ethanolic clove NP	Ethanolic Ash NP	Positive control antibiotic
	13	14	20
	15	20	20
	16	18	21
	14	19	22
	14.50 ± 0.64	17.75 ± 1.31	20.75 ± 0.47

Table 2: Antibacterial activity against *E. coli*	Ethanolic clove NP	Ethanolic Ash NP	Positive control antibiotic
	15	15	23
	18	18	16
	16	17	18
	15	16	20
	16.0000 ± 0.7071	16.5000 ± 0.6455	19.2500 ± 1.4930

Table 3: Antibacterial activity against *Pseudomonas*	Ethanolic clove NP	Ethanolic Ash NP	Positive control antibiotic
	13	15	22
	14	15	20
	11	14	21
	10	14	20
	12.00± 0.91	14.50 ± 0.28	20.75 ± 0.47

Table 4: Antibacterial activity against *Streptococcus*	Ethanolic clove NP	Ethanolic Ash NP	Positive control antibiotic
	15	8	20
	20	20	15
	19	18	20
	12	14	18
	16.50 ± 1.84	15.00 ± 2.64	18.25 ± 1.18

References

1. Thibier M, Guerin B. 2000. Hygienic aspects of storage and use of semen for artificial insemination. Anim Reprod Sci. 62(open in a new window)(–13(open in a new window)):233–251.

2. Ong, C. T., Turni, C., Blackall, P. J., Boe-Hansen, G., Hayes, B. J., and Tabor, A. E. (2021). Interrogating the bovine reproductive tract metagenomes using culture-independent approaches: a systematic review. *Anim. Microbiome* 3:41. doi: 10.1186/s42523-021-00106-3

3. Marcus S, Bernstein M, Ziv G, Glickman A, Gipps M. 1994. Norfloxacin nicotinate in the treatment of Pseudomonas aeruginosa infection in the genital tract of a bull. Vet Res Commun. 5:331–336. doi:https://doi.org/10.1007/BF01839283(open in a new window)

4. Rana N, Vaid RK, Phulia SK, Singh P. 2012. Assessment of bacterial diversity in fresh bubaline semen. Indian J Anim Sci. 82(6):596–598

5. Wierzbowski S. 1981. Bull semen opportunistic pathogen and ubiquitary microflora. In: Disease control in semen and embryos. FAO. Rome (Italy); p. 21–28.

6. Hare WCD. 1985. Diseases transmissible by semen and embryo transfer techniques. In: Office international des épizooties, Technical Series No 4, Paris. Vol. 4. p. 1–83.

7. Althouse GC, Pierdon MS, Lu KG. 2008. Thermotemporal dynamics of contaminant bacteria and antimicrobials in extended porcine semen. Theriogenology. 70(open in a new window)(8(open in a new window)):1317–1323. doi:https://doi.org/10.1016/j.theriogenology.2008.07.010(open in a new window).

8. Bussalleu E, Yeste M, Sepúlveda L, Torner E, Pinart E, Bonet S. 2011. Effects of different concentrations of enterotoxigenic and verotoxigenic E. coli on boar sperm quality. Anim Reprod Sci. 127(open in a new window)(–34(open in a new window)):176–182. doi:https://doi.org/10.1016/j.anireprosci.2011.07.018(open in a new window).

9. Köhn FM, Erdmann I, Oeda T, El Mulla KF, Schiefer HG, Schill WB. 1998. Influence of urogenital infections on sperm functions. Andrologia. 30(open in a new window)(S1(open in a new window)):73–80. doi:https://doi.org/10.1111/j.1439-0272.1998.tb02829.x(open in a new window).

10. Monga M, Robert JA. 1994. Sperm agglutination by Bacteria: receptor-Specific Interactions. J Androl. 15(2):151–156.

11. Fraczek M, Kurpisz M. 2015. Mechanisms of the harmful effects of bacterial semen infection on ejaculated human spermatozoa: potential inflammatory markers in semen. Folia HistochemCytobiol. 53(open in a new window)(3(open in a new window)):201–217. doi:https://doi.org/10.5603/fhc.a2015.0019(open in a new window).

12. Shahid, Hussain, Abro., Rani, Abro., Rahamatullah, Rind., Asghar, Ali, Kamboh., Akeel, Ahmed, Memon., Hassina, Baloch., Bakhtawar, Wagan. (2016). Antibiogram of the Micrococcus luteus, Pseudomonas aeruginosa, Staphylococcus epidermidis and Staphylococcus intermedius isolated from the bovine frozen semen.

13. G.S., Meena., M., Bhakat., V., S., Raina., A.K., Gupta., Tushar, Kumar, Mohanty., Rohit, Bishist. (2017). Effect of different antibiotic combinations in extender on bacterial load and seminal characteristics of Murrah bulls. Buffalo Bulletin, 36(1):251-257.

14. Luis, O., Alba, Gómez., Enrique, A., Silveira, Prado. (2005). Perdurabilidad de la efectividad de la combinaciónpenicilina-estreptomicinaen la reducción de la cargabacteriana del semen de toro congeladoen pastillas (Durability of the effectiveness of the penicillin-streptomycin combination in the reduction of the bacterial content of frozen bulls semen in concentrated pellet form).

15. J., M., Morrell., Aleksandar, Cojkić., P., Malaluang., Theodoros, Ntallaris., Johanna, Lindahl., Ingrid, Hansson. (2024). Antibiotics in semen extenders - a multiplicity of paradoxes.. Reproduction, Fertility and Development, doi: 10.1071/rd23218

16. K., L., Goularte., Flávia, L., S., Voloski., Josiara, F., M., Redú., C., E., R., Ferreira., A., D., Vieira., Eduarda, Hallal, Duval., Rafael, Gianella, Mondadori., Thomaz, Lucia. (2020). Antibiotic resistance in microorganisms isolated in a bull semen stud.. Reproduction in Domestic Animals, 55(3):318-324. doi: 10.1111/RDA.13621

17. N.H., Liversedge., Julian, M., Jenkins., Stephen, D., Keay., Eileen, A., McLaughlin., H., Al-Sufyan., L., A., Maile., L.A, Joels., Michael, G.R., Hull. (1996). Antibiotic treatment based on seminal cultures from asymptomatic male partners in in-vitro fertilization is unnecessary and may be detrimental. Human Reproduction, 11(6):1227-1231. doi: 10.1093/OXFORDJOURNALS.HUMREP.A019361

18. Aleksandar, Cojkić. (2023). Identification of bull semen microbiota and possible alternatives for antibiotics in semen extenders. Acta Universitatis AgriculturaeSueciae, doi: 10.54612/a.4al7k99m30

19. Shiza, Nasreen., Muhammad, Amjad, Awan., Asma, Ul-Husna., Bushra, Allah, Rakha., Muhammad, Sajjad, Ansari., William, V., Holt., Shamim, Akhter. (2020). Honey as an Alternative to Antibiotics for Cryopreservation of Nili-Ravi Buffalo Bull Spermatozoa. Biopreservation and Biobanking, 18(1):25-32. doi: 10.1089/BIO.2019.0054

20. Keeratikunakorn, K., Chanapiwat, P., Aunpad, R., Ngamwongsatit, N., &Kaeoket, K. (2024). Effect of Antimicrobial Peptide BiF2_5K7K on Contaminated Bacteria Isolated from Boar Semen and Semen Qualities during Preservation and Subsequent Fertility Test on Pig Farm. *Antibiotics*, *13*(7), 579.

21. Kanwar, A., Virmani, M., Lal, S., Chaudhary, K., Kumar, S., Magotra, A., & Pandey, A. K. (2023). Silver nanoparticle as an alternate to antibiotics in cattle semen during cryopreservation. *Animal Reproduction*, *20*, e20220030.

22. A.S., Vickram., Kuldeep, Dhama., Archana, K., R., Parameswari., Ramesh, Pathy, M., Hafiz, M.N., Iqbal., Sridharan, T, B. (2017). Antimicrobial peptides in semen extenders: a valuable replacement option for antibiotics in cryopreservation - a prospective review.. Journal of Experimental Biology and Agricultural Sciences, 5(5):578-588. doi: 10.18006/2017.5(4).578.588

23. Oleksandra, Tul., Borys, Kyrychko., T., G., Panasova. (2022). Modern technologies for storing semen of domestic animals without the addi-tion of antibiotics. Scientific Messenger of LNU of Veterinary Medicine and Biotechnology, 24(106):74-80. doi: 10.32718/nvlvet10612

24. Salem S.S., Fouda A. Green synthesis of metallic nanoparticles and their prospective biotechnological applications: An overview. Biol. Trace Elem. Res. 2021;199:344–370. doi: 10.1007/s12011-020-02138-3.

25. Akter S., Huq M.A. Biologically rapid synthesis of silver nanoparticles by Sphingobium sp. MAH-11 T and their antibacterial activity and mechanisms investigation against drug-resistant pathogenic microbes. Artif. Cells Nanomed. Biotechnol. 2020;48:672–682. doi: 10.1080/21691401.2020.1730390

26. Huq M.A., Akter S. Bacterial mediated rapid and facile synthesis of silver nanoparticles and their antimicrobial efficacy against pathogenic microorganisms. Materials. 2021;14:2615. doi: 10.3390/ma14102615.

27. Clogston, J. D., & Patri, A. K. (2011). Zeta potential measurement. *Methods in molecular biology (Clifton, N.J.)*, *697*, 63–70. https://doi.org/10.1007/978-1-60327-198-1_6

28. Ali, A., Mir, G.J., Ayaz, A., Maqbool, I., Ahmad, S.B., Mushtaq, S., Khan, A., Mir, T.M. and Rehman, M.U., 2023. In silico analysis and molecular docking studies of natural compounds of Withaniasomnifera against bovine NLRP9. *Journal of Molecular Modeling*, *29*(6), p.171

29. Ahmad, N., Malik, M. A., Wani, A. H., & Bhat, M. Y. (2024). Biogenic Silver Nanoparticles from Fungal Sources: Synthesis, Characterization, and Antifungal Potential. *Microbial Pathogenesis*, 106742.

30. Akshay, V. R., Vasundhara, M., & Muthu, A. (2020). Biosynthesis of multiphase iron nanoparticles using Syzygium aromaticum and their magnetic properties. *Colloids and Surfaces A: Physicochemical and Engineering Aspects*, *603*, 125241.

31. Joshi, N., Jain, N., Pathak, A., Singh, J., Prasad, R., & Upadhyaya, C. P. (2018). Biosynthesis of silver nanoparticles using Carissa carandas berries and its potential antibacterial activities. *Journal of Sol-Gel Science and Technology*, *86*, 682-689.

32. Manoja, Kumar, Das., Danda, P., Acharya., Malati, Hembrom., I, M, Nagendra, Nayak. (2024). Biosynthesis of silver nanoparticles using cow dung extract and evaluation of their antibacterial potentials. Microbes and Infectious Diseases (Print), 0(0):0-0. doi: 10.21608/mid.2024.281553.1879

33. Nasser, Nafaa, Abrahem, Alqurashy. (2024). Green synthesis of silver nanoparticles using sunflower extract for biological application. International journal of biology sciences, 6(1):193-200. doi: 10.33545/26649926.2024.v6.i1c.205

34. Tavan, M., Hanachi, P., Mirjalili, M. H., & Dashtbani-Roozbehani, A. (2023). Comparative assessment of the biological activity of the green synthesized silver nanoparticles and aqueous leaf extract of Perilla frutescens (L.). *Scientific Reports*, *13*(1), 6391.

35. Aakash, Kumar., Madhusudan, Kr., Mahto., Shalu, Priya., S.S., Thakur., Priyanka, Paramanik., Renuka, Verma., Padmabati, Mahato., Abhijeet, Bera. (2024). A comprehensive review of green synthesis, characterization and biomedical applications of silver nanoparticle synthesized using plant extracts. World Journal Of Advanced Research and Reviews, 22(3):1950-1977. doi: 10.30574/wjarr.2024.22.3.1899

36. Dubey, S., Virmani, T., Yadav, S. K., Sharma, A., Kumar, G., & Alhalmi, A. (2024). Breaking Barriers in Eco-Friendly Synthesis of Plant-Mediated Metal/Metal Oxide/Bimetallic Nanoparticles: Antibacterial, Anticancer, Mechanism Elucidation, and Versatile Utilizations. *Journal of Nanomaterials*, *2024*(1), 9914079.

37. R., Prakruthi., H., N., Deepakumari., H., D., Revanasiddappa., Faisal, M., Alfaisal., Shamshad, Alam., Hasan, Sh., Majdi., Mohammad, Amir, Khan., Shareefraza, J., Ukkund. (2024). Silver vanadate nanoparticles: Green synthesis, enhanced photocatalytic and antibacterial activity. AIP Advances, 14(8) doi: 10.1063/5.0217829

38. Valgas, C., Souza, S. M. D., Smânia, E. F., &Smânia Jr, A. (2007). Screening methods to determine antibacterial activity of natural products. *Brazilian journal of microbiology*, *38*, 369-380.

39. Aisha, Mohammed, Al-amri., Awatif, Hindi. (2024). Green Silver nanoparticles as Anticancer and antibacterial agent. doi: 10.21608/ajsr.2024.352905

40. Rai, M., Yadav, A., & Gade, A. (2009). Silver nanoparticles as a new generation of antimicrobials. Biotechnology Advances, 27(1), 76-83.

41. Ahmed, S., Ahmad, M., Swami, B. L., & Ikram, S. (2016). A review on plants extract mediated synthesis of silver nanoparticles for antimicrobial applications: A green expertise. Journal of Advanced Research, 7(1), 17-28.

42. Morones, J. R., Elechiguerra, J. L., Camacho, A., Holt, K., Kouri, J. B., Ramírez, J. T., &Yacaman, M. J. (2005). The bactericidal effect of silver nanoparticles. Nanotechnology, 16(10), 2346.

43. Diana, Maria, Dégi., Katalin, Lányi., F., Beteg., V., Herman., J., Dégi., Sorın, Morariu., Флорин, Муселин. (2024). Green synthesized silver nanoparticles using Sempervivum tectorum extract have an antibacterial effect against Staphylococcus pseudintermedius isolated from a dog's otitis externa. doi: 10.21203/rs.3.rs-4382878/v1

